Original Article

JCBFM

Journal of Cerebral Blood Flow & Metabolism
2016, Vol. 36(10) 1731–1743

DOI: 10.1177/0271678X16630556
jcbfm.sagepub.com
SAGE

Transient increase of fractional anisotropy in reversible vasogenic edema

Shihoko Kimura-Ohba[1], Yi Yang[1], Jeffrey Thompson[1], Tomonori Kimura[2], Victor M Salayandia[1], Melissa Cosse[1], Yirong Yang[3], Laurel O Sillerud[1,3] and Gary A Rosenberg[1,4,5]

Abstract

Brain vasogenic edema, involving disruption of the blood-brain barrier, is a common pathological condition in several neurological diseases, with a heterogeneous prognosis. It is sometimes reversible, as in posterior reversible encephalopathy syndrome, but often irreversible and our current clinical tools are insufficient to reveal its reversibility. Here, we show that increased fractional anisotropy in magnetic resonance imaging is associated with the reversibility of vasogenic edema. Spontaneously, hypertensive rats-stroke prone demonstrated posterior reversible encephalopathy syndrome-like acute encephalopathy in response to high-dose cyclosporine A treatment; the deteriorating neurological symptoms and worsening scores in behavioral tests, which were seen in acute phase, dissappered after recovery by cessation of cyclosporine A. In the acute phase of encephalopathy, the fractional anisotropy and apparent diffusion coefficient increased in areas with IgG leakage. This increase of fractional anisotropy occurred in the absence of demyelination: fluid leakage into the myelinated space increased the axial, but not the radial, diffusivity, resulting in the increased fractional anisotropy. This increased fractional anisotropy returned to pre-encephalopathy values in the recovery phase. Our results highlight the importance of the fractional anisotropy increase as a marker for the reversibility of brain edema, which can delineate the brain areas for which recovery is possible.

Keywords

Blood-brain barrier, brain vasogenic edema, diffusion tensor imaging, fractional anisotropy, posterior reversible encephalopathy syndrome

Received 4 September 2015; Revised 21 December 2015; Accepted 11 January 2016

Introduction

Brain edema, a fundamental and universal pathological condition of neurological diseases, is classified into two types: vasogenic and cytotoxic. Brain vasogenic edema results after the disruption of the blood-brain barrier (BBB), whereas cytotoxic edema is caused by cellular swelling of neurons or astrocytes due to abnormal fluxes of sodium and other ions.[1] The lesions where the two types of edema coexist are likely to develop permanent damage.[2]

Whether or not the vasogenic edema is reversible strongly influences the prognosis for patients. When vasogenic edema occurs in multiple sclerosis and small vessel disease, the edema is irreversible and the prognosis is mainly unfavorable,[3,4] while in the posterior reversible encephalopathy syndrome (PRES) the prognosis is usually favorable.[5] PRES is unique in that it is one of a few diseases which present with only vasogenic edema and whose clinical course is usually reversible. The over-dose usage of certain drugs, such as cyclosporine A (CsA) in the presence of hypertension, is a risk factor for the occurrence of

[1]Department of Neurology, University of New Mexico, Albuquerque, USA
[2]Department of Molecular Genetics and Microbiology, University of New Mexico, Albuquerque, USA
[3]BRaIN Imaging Center and College of Pharmacy, University of New Mexico, Albuquerque, USA
[4]Department of Neurosciences, University of New Mexico, Albuquerque, USA
[5]Department of Cell Biology and Physiology, University of New Mexico Health Sciences Center, Albuquerque, New Mexico, USA

Corresponding author:
Shihoko Kimura-Ohba, Department of Neurology, Health Science Center, University of New Mexico, MSC11 6035, Domenici Hall/NRF, 1101 Yale Blvd. NE, Albuquerque, NM 87106-3834, USA.
Email: ShKimura@salud.unm.edu and skimura@ped.med.osaka-u.ac.jp

PRES; endothelial injury, vasoconstriction, and increasing vascular permeability induced by CsA predisposes patients at risk to PRES.[5–7]

Magnetic resonance (MR) imaging plays a key role in the assessment of brain lesions in clinical practice because the imaging sequences can be tailored to measure many of the physical properties of tissue water. For example, the random movement of water molecules (Brownian motion) can be qualitatively determined by diffusion-weighted imaging (DWI) or the apparent diffusion coefficient (ADC) can be quantitatively determined in vivo. The increases in the ADC values in MR images are used for the diagnosis of vasogenic edema, but the values of the ADC do not correlate with the prognosis.[8] The prognosis of vasogenic edema is heterogeneous as described above and its reversibility cannot be predicted using current clinical tools; therefore, we need more specific and advanced methods of magnetic resonance imaging (MRI) to predict the prognosis of vasogenic edema.

Since the brain contains oriented fibers, which impose anisotropy on water diffusion, MRI of the components of the diffusion tensor is an important technique for the quantitative evaluation of white matter injury.[9] This diffusion tensor imaging (DTI) has recently moved into clinical practice,[10–13] with particular attention being paid to measurements of the fractional anisotropy (FA) of water diffusion in the brain. Water molecules diffuse freely in all directions (*isotropically*) in a random manner in an unstructured space such as in the fluid within the cerebral ventricles, resulting in a low value (near zero) for the FA. In anisotropic brain white matter tracts, however, FA values are higher (closer to 1, indicating greater anisotropy) due to relatively unrestricted diffusion of water molecules parallel to the axons but with restricted diffusion perpendicular to the axons.[14] It is generally accepted that an FA decrease indicates demyelination and/or axonal injury in white matter, and is associated with a poor prognosis.[15] On the other hand, an FA increase has been reported to reflect axonal regeneration, plasticity, or gliosis.[15] However, since the prognostic value of FA measurements has not yet been evaluated, we believed that measuring the FA during and after vasogenic edema was of potential interest.

In this work, we showed that an FA increase was observed during vasogenic edema. By establishing an animal model (acute reversible encephalopathy (ARE)) for reversible vasogenic edema, we found that vasogenic edema induces an FA increase only when myelin structures are conserved. As a result, an FA increase during vasogenic edema was found to be a marker for potential recovery not only in PRES but also in the other neurological diseases, which present vasogenic edema, whereas an FA decrease was associated with chronic brain injury.

Materials and methods

Animal experiment

The animal protocol was approved by the Institutional Animal Care and Use Committee (IACUC) at the University of New Mexico and followed the NIH Policy on Humane Care and Use of Laboratory Animals. All animal experiments followed the ARRIVE guidelines. To establish ARE model, 7-week-old spontaneously hypertensive, stroke-prone (SHR-SP) rats were fed the Japanese permissive diet (JPD; 16% protein, 0.75% potassium, 4.0% sodium; Ziegler Bros, Inc.) with 1% sodium chloride added to drinking water. At 9 weeks of age, they were randomly divided into two groups and injected intraperitoneally either with Cyclosporine A (CsA, Santa Cruz, TX, USA), dissolved in olive oil, or olive oil as vehicle, once daily for 2 days. To induce neurological symptoms, the doses of CsA (200 mg/kg/day) were set higher than those of the CsA nephrotoxicity rodent model according to our preliminary studies.[16,17] To investigate recovery from the ARE model, CsA injections and the JPD were discontinued on day 2, and rats were fed a regular diet with tap water for a week. The unilateral carotid arterial occlusion (UCAO)-JPD model was generated as previously described[18] and used herein as a model for chronic and irreversible vasogenic edema. The middle cerebral artery occlusion (MCAO) model was generated as previously described and used as a positive control for Fluoro-Jade staining.[19]

Measurement of physiological parameters

The body weights of both the ARE and control group rats were measured in daily basis. Systolic and diastolic blood pressures (SBP and DBP) were measured at two points; before starting the JPD and before starting the CsA or vehicle injections to confirm that the rats SBPs were above 200 mmHg, which is the physiological mean value for SHR-SP. Non-invasive blood pressure measurements were taken with a tail-cuff using the CODA system (Kent Scientific Inc., CT, USA). Mean values of the blood pressure were calculated from seven measurements.

Neurological and behavioral testing

Neurological performance was assessed by clinical scoring of neuromuscular function,[20] daily Rotor-rod treadmill system tests (San Diego Instruments, CA, USA) and twice-weekly Catwalk XT (Noldus, CA, USA) experiments. Neurological symptoms were also assessed by the observation of seizures. The rotor-rod treadmill system tests were performed to detect motor

deficits. Prior to the start of CsA treatments, rats were trained on the Rotor-rod cylinder and the latency to fall from the rod was averaged in three trials. Speed was gradually increased from 5 to 40 rpm within 5 min. The CatWalk XT was used to detect subtle gait and motor impairment.[21–23] Prior to the start of the CsA treatments, the rats were trained to walk along the walkway in a dark room. Then, rats were subjected to gait assessment at days 0 and 2 for all animals, and day 9 for the recovery animals. One trial consisted of at least three runs and three successfully recorded runs were counted for analysis. We performed analyses for stance duration, stride length, and body speed for each of four paws.

Histological analysis

Histological analyses were prepared as previously described.[18] In brief, rats were anesthetized with pentobarbital (50 mg/kg, intraperitoneally) and transcardially perfused with 2% Periodate Lysine Paraformaldehyde (PLP; 2% paraformaldehyde, 0.1 mol/L sodium periodate, 0.075 mol/L lysine in 100 mmol/L phosphate buffer, pH 7.3). Brains were removed, equilibrated to 2% PLP, cryoprotected with 30% sucrose, and embedded in OCT compound (Sakura Finetek, CA, USA) using 2-methylbutane cooled in liquid nitrogen. Brain tissues were then sectioned at 10 μm thickness. Kluver-Barrera (K&B) and Hematoxylin-Eosin (H&E) staining followed standard protocols. A TACS® 2 TdT DAB Kit (Trevigen Inc., MD, USA) was used for TUNEL (terminal deoxynucleotide transferase–mediated deoxyuridine triphosphate nick-end labeling) staining and Fluoro-Jade C (Histo-Chem Inc.) was used for Fluoro-Jade staining.[24] For immunohistochemistry, brain sections were stained using the following antibodies; rat anti-endothelial cell antibody-1 (RECA-1; 1:300, Abcam, MA, USA), glial fibrillary acidic protein (GFAP; 1:400, Sigma, MO, USA), anti CD11b (OX-42; 1:400, Accurate, NY, USA), myelin basic protein (MBP; 1:1000, Covance, CA, USA), and anti-Cy-3-conjugated affinity pure goat anti-rat IgG (1:50, Jackson Immuno Research Laboratories Inc., PA, USA).

MRI and analysis

All animals underwent acute-phase MRI, and the recovery groups also underwent recovery phase MRI. MRI was performed on a 4.7 Tesla, 40 cm bore Bruker Biospec system, equipped with a 12 cm shielded gradient coil. Rats were placed prone on an animal bed, which was supported from the table outside the magnet. A 72-mm volume coil with a 2.5 cm actively decoupled brain surface coil was used for excitation and signal detection, respectively. Initial localizer images were acquired using a two-dimensional (2D) fast low-angle shot (FLASH) sequence with TR/TE 100/6 ms, matrix 128×128, FOV $8\,\text{cm} \times 8\,\text{cm}$, and one slice per orientation. Then, T_2-weighted (T_2w) MRI was performed using the following parameters: 2D rapid acquisition with relaxation enhancement (RARE), TR/TE 5000/65 ms, FOV $4\,\text{cm} \times 4\,\text{cm}$, slice thickness 1 mm, slice gap 1.1 mm, number of slices 12, matrix 256×256, number of averages 4. Magnetic resonance angiography (MRA) data were acquired using a FLASH-3D sequence, TR/TE 15/3 ms, matrix $256 \times 256 \times 128$, number of average $= 1$. Diffusion tensor MR images were obtained using echo-planar, diffusion tensor imaging (EP-DTI) sequences with a TR of 3000 ms, a TE of 40 ms, and a b-value of $2000\,\text{mm}^2/\text{s}$ with 30 diffusion gradient directions.

The acquired MR data were transferred to a dedicated computer workstation for post processing. ADC maps were generated from the raw DTI data to identify increased tissue water, which could be quantified as an increase in the ADC. FA, axial diffusivity (AD), radial diffusivity (RD), and mean diffusivity maps were calculated from the raw DTI data using ParaVision 5.1 (Bruker Biospin, Billerica, CA, USA). The areas of FA and ADC increase were determined from each of the slices. FA and ADC values in the white and gray matter were calculated in the slice that showed the largest changes for the CsA acute animals and these values were compared with the values from the same area and same slices from the CsA recovery and control animals. MRA 3D data were processed with ParaVision 5.1. Vessel areas (pixels) in 3D images from both CsA acute and control animals were calculated.

Statistics

A two-tailed Student's *t*-test was used for determining the significance of differences between two groups, while a one-way ANOVA was used for multiple different groups. Occurrence of seizures was assessed by Kaplan–Meier analysis and differences were determined by the log rank test. Principal component analysis (PCA) and its related biplot analysis, were performed as described previously.[25] Data were presented as mean and SEM. Statistical significance was defined as $P < 0.05$.

Results

Establishment of a rodent ARE model

An ARE model was established in rodents according to the protocol shown in Figure 1(a). The ARE animals lost weight until 4 days after the cessation of the

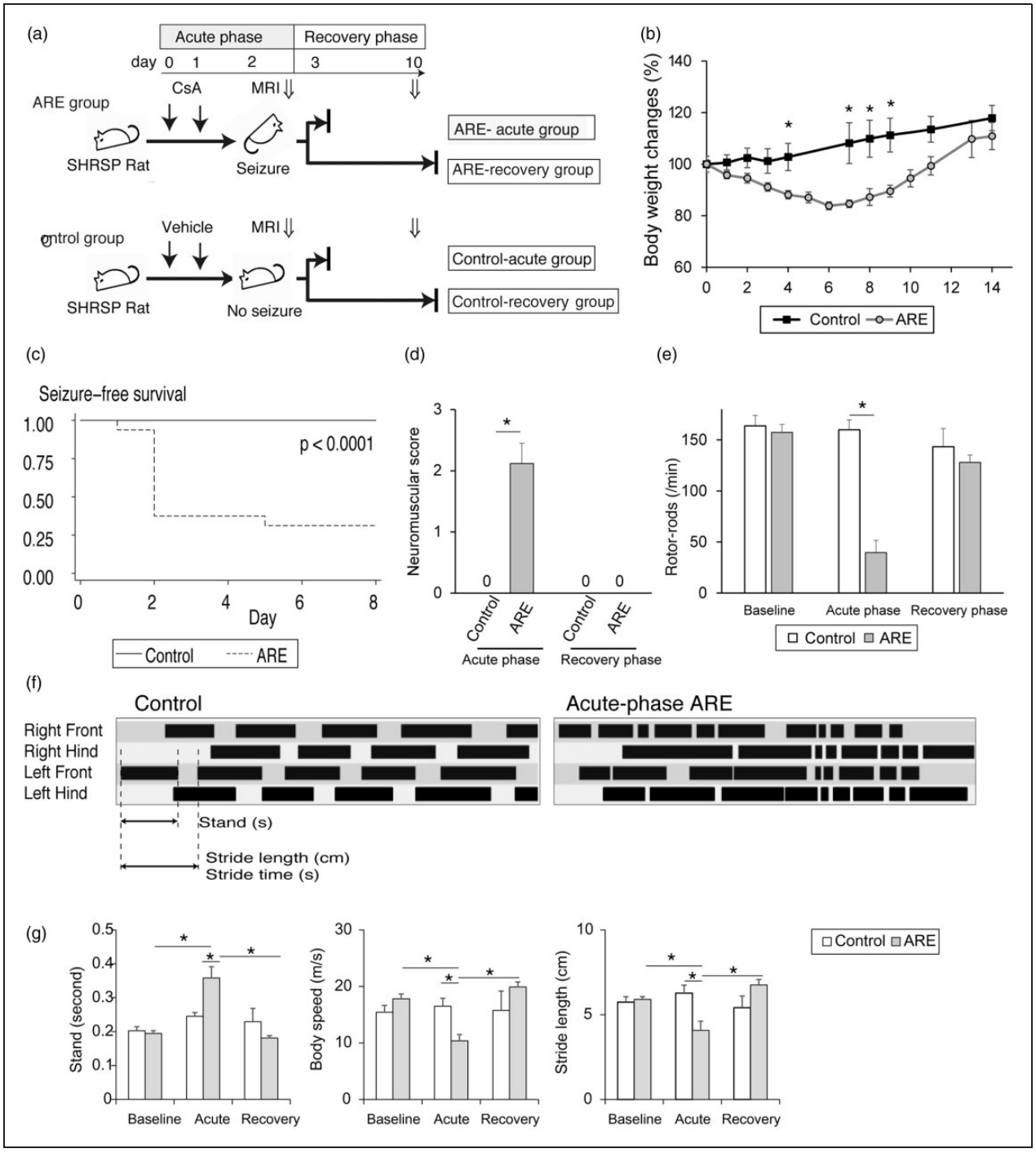

Figure 1. Establishment of a rodent ARE model. (a) Protocol for inducing ARE in rats. SHR-SP rats fed the JPD were treated with overdose cyclosporine A once daily for 2 days. Brain MRI was taken on day 3. CsA injection and JPD were discontinued to induce recovery, and the recovery-phase MRI was taken on day 10. (b) Body weight changes of ARE model rats and their control. (c) Kaplan–Meier analysis for the occurrence of seizure. (d, e) Neurological scores (d) and rotor-rods latencies (e) of ARE model rats and their control at baseline, and during the acute- and recovery-phase. (f) Representative timing views of foot prints from an acute-phase ARE rat and its control analyzed by CatWalk XT. Parameters used in (g) are shown. (g) Stand time, body speed, and stride length of ARE model rats and their control at baseline, and during the acute- and recovery-phase. Data from left hinds are shown. Data, means ± SE, n = 8 to 16, $^*P < 0.05$.

ARE: acute reversible encephalopathy; SHR-SP: spontaneously hypertensive, stroke-prone; JPD: Japanese permissive diet; MRI: magnetic resonance imaging; CsA: cyclosporine A.

injections when they started to gain weight, whereas control group animals gained weight throughout the experimental period (Figure 1(b)). The mean systolic blood pressure was found to be 160 mmHg for both the ARE and control group animals before the initiation of the JPD; this increased to 230 mmHg after the initiation of the JPD, but before the CsA injections in both two groups (data not shown). Sixty-five percent of the ARE animals had seizures in the acute-phase, and most of these seizures occurred on day 2 (Figure 1(c)). All of the ARE animals displayed neurological symptoms, while there were no neurological symptoms in the control animals (Figure 1(d)). Rotorrod latency was significantly decreased during the acute-phase of the ARE animals compared with the controls (Figure 1(e)). Catwalk timing views revealed that walking patterns were impaired in the ARE acute animals compared with the control animals (Figure 1(f) and Supplementary Movie 1). Further analyses showed that stand time was prolonged, and that both body speed and stride length decreased in all 4 paws in ARE animals compared with the control group animals. (Figure 1(g) for left hinds; data not shown for the other 3 paws.) These symptoms and test scores all resolved during the recovery-phase, in which animals did not receive any further doses of drug and were returned to the normal diet regimen (Figure 1(d) to (g)). Thus, the encephalopathy produced in this rodent ARE model was found to be reversible.

Brains of ARE model showed a reversible increase of FA

We next used MRI to examine the brain lesions produced in the ARE model. Both the FA and the ADC were seen to increase in acute-phase ARE animals (acute ARE) compared with control animals (Figure 2(a), left and middle columns). Although visual inspection of the T_2w MR images did not show apparent changes in the MR signal intensities (Figure 2(a), right column), measurements of the pixel intensities revealed a statistically significant intensity increase in the brains of the acute ARE animals compared with the controls (data not shown) consistent with the induction of vasogenic edema in the ARE model. The ARE lesions were diffuse but were concentrated in MR slices 4 to 7 mm posterior to the Bregma, which are locations of the visual, auditory, and motor cortices. An FA increase was seen in almost the entire white and gray matter (Figure 2(a)). The observed ADC increase suggested the presence of vasogenic edema (Figure 2(a) and (d)). These increases in FA and ADC seen in acute-phase ARE animals resolved in the recovery phase (recovery ARE, Figure 2(a) lower column).

The MRI signals were quantified in each region of white and gray matter in both hemispheres. The increased FA seen in the acute ARE animals was confirmed in all the areas assessed (Figure 2(b)). These FA values returned to normal in the recovery phase of the ARE model. The ADC values increased in all regions of the brains during acute ARE, reaching statistical significance in 6/8 regions (Figure 2(d)) and these changes returned to normal during the recovery phase of the ARE model (Figure 2(d)). These results suggest that both the FA and ADC values sensitively respond to ARE; these values increase in acute ARE and normalize after recovery.

Our observation that the diffusion properties of brain water return to normal supports the concept that the type of vasogenic edema seen in the ARE model is reversible. It was of great interest, therefore, to also examine an irreversible type of vasogenic edema. We compared the FA/ADC values of our ARE model with those from a chronic white matter injury model (UCAO-JPD animals) as a representative of irreversible vasogenic edema.[18,26] The UCAO-JPD model has previously been shown to produce irreversible IgG leakage and demyelination in the corpus callosum (CC).[18,26] As expected, we saw a large increase of the ADC in the UCAO-JPD animals, suggesting the presence of vasogenic edema (Figure 2(e)). On the contrary, the FA decreased in UCAO-JPD animals (Figure 2(c)). These results suggested that an FA increase is specifically seen in the acute-phase of reversible vasogenic edema.

MRA of the acute ARE animals revealed vasoconstriction and a narrowing of the distal vessel branches compared with the control animals (Figure 3(a)) The areas of the vascular beds in acute ARE were significantly smaller than those of control animals (Figure 3(b)). These changes were comparable to human CsA-induced encephalopathy.

Brain lesions of ARE model revealed IgG leakage without apparent demyelination

We next performed a histological examination of the brain lesions of the ARE model animals. IgG leakage was detected within the injured area identified by MRI of acute-phase ARE (Figure 4(a) and (b), middle columns), while H&E staining indicated a lack of hemorrhages (Supplementary Figure 1(A)). No apparent demyelination was observed in the acute ARE model, as assessed by MBP and K&B staining (Figure 4(c) and Supplementary Figure 1(B), middle columns). Furthermore, Fluoro Jade and TUNEL staining showed neither neuronal degeneration nor apoptotic cells in the brains from the acute ARE rats (Figure 4(d) and (e)). In line with previously reported PRES cases,[27] a slight astrocytosis was observed in the

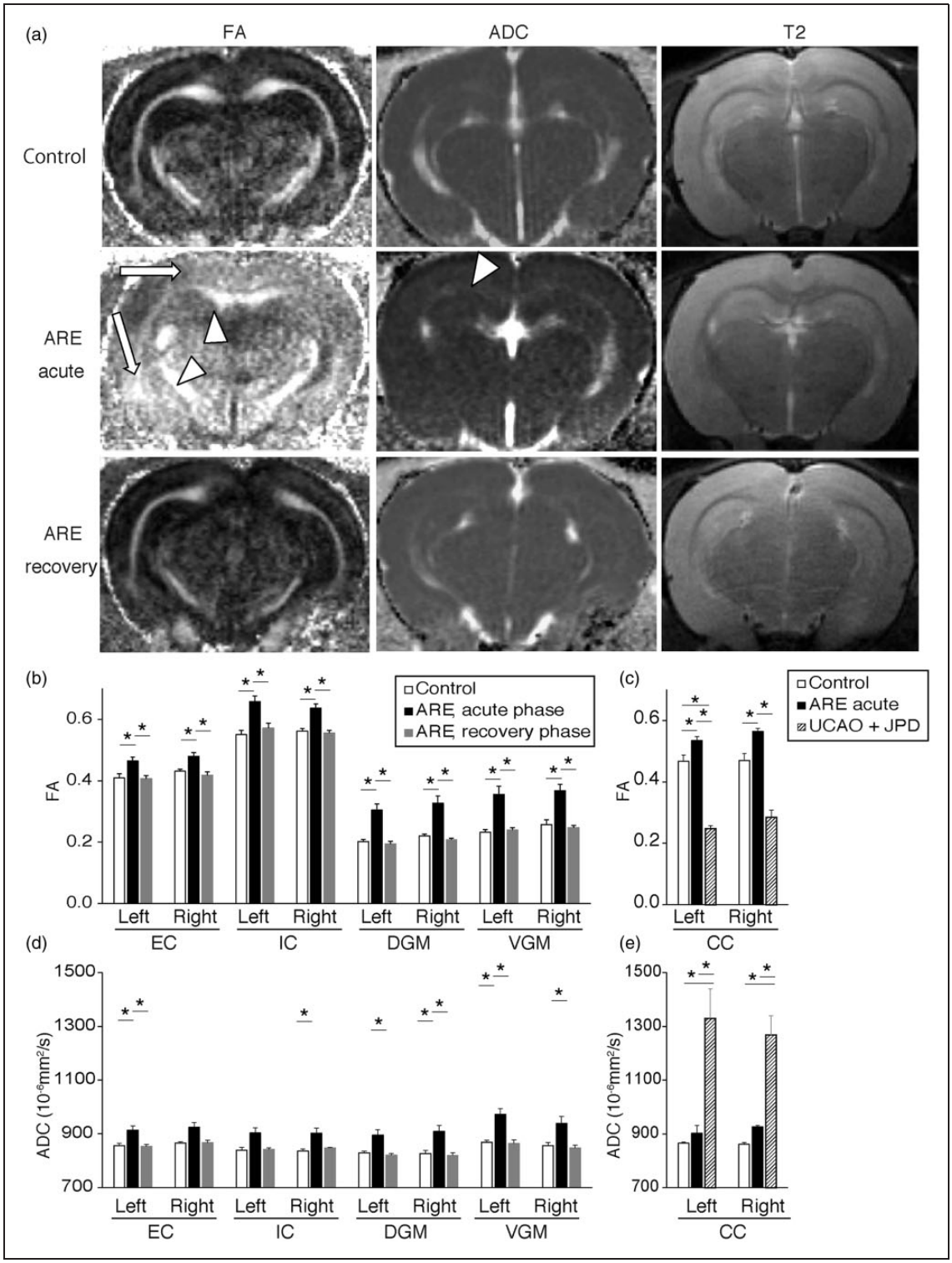

Figure 2. Brains of ARE model show a reversible increase of FA. (a) Brain MRI (FA, ADC, and T2 images) from acute- and recovery-phase of ARE model and their controls. Arrows and arrowheads indicate areas of increased FA in dorsal and ventral gray matter (DGM and VGM), and areas where both the FA and ADC increased in CC and internal capsule (IC), respectively. (b–e) FA (b and c) and ADC (d and e) values in white matter and gray matter of acute- and recovery-phase ARE, unilateral carotid arterial occlusion on JPD (UCAO-JPD), and control. Because main lesions of UCAO-JPD were restricted to the corpus callosum, the comparison between acute ARE, UCAO-JPD, and control were separately shown in C and E. Data, means ± SE, n = 4 to 16, $^*P < 0.05$.

ARE: acute reversible encephalopathy; MRI: magnetic resonance imaging; FA: fractional anisotropy; ADC: apparent diffusion coefficient; CC: corpus callosum; DGM: dorsal gray matter; VGM: ventral gray matter; UCAO-JPD: unilateral carotid arterial occlusion–Japanese permissive diet; EC: external capsule.

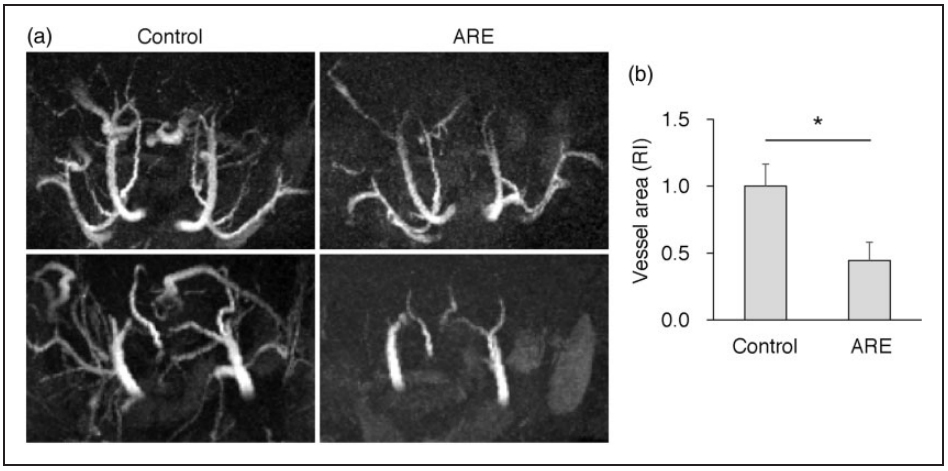

Figure 3. MRA of ARE acute animals revealed vasoconstriction and narrowing of distal branch arteries. (a) 3D MRA image of acute-phase ARE and its control. (b) Relative area of vascular beds in acute-phase ARE and its control. Data, means ± SE, n = 4, $^*P < 0.05$. MRA: magnetic resonance angiography; ARE: acute reversible encephalopathy; RI: relative index.

acute ARE model and also in recovery ARE compared with those of the controls, as assessed by GFAP staining. These astrocytes were morphologically radial and did not show the cellular-ballooning (Supplementary Figure 1(C)). A slight microglial activation was also seen in control animals as well as both acute and recovery ARE animals, because the control animals were also fed the JPD. Morphologically, the microglia in acute ARE animals were indifferently rod-shaped or radial, and none of these cells were ballooning (Supplementary Figure 1(D)). The IgG leakage resolved and no further adverse histological findings were observed in the recovery-phase of the ARE model (Figure 4(a) and (b), left column). The mild astrocytosis and microglial activation did not resolve in spite of the reversal of the IgG leakage. These results suggested that the brain lesions of the ARE model constitute a reversible vasogenic edema (Figure 4(f)) without detectable demyelination, hemorrhage, or cell death.

Increased axial, but not radial, diffusivity due to IgG leakage is the cause of FA increase in acute ARE

Since the increases in the ADC and in the leakage of IgG both result from a compromise in the integrity of the BBB, we expected that these two disparate measures should be correlated. Potential correlations between the MRI and histological findings were investigated by measuring the ADC in the MRI slices and the IgG leakage areas in MRI-matched brain slices. IgG leakage occurred broadly in white matter tracts in both the acute ARE and UCAO-JPD models. IgG leakage was positively correlated with the ADC increase in both the acute ARE and UCAO-JPD models (Figure 5(a)). However, the FA values changed in opposite directions in these two models: the FA increase seen in the acute ARE model totally distinguished this model from the UCAO-JPD model where the FA was found to decrease (Figure 5(b)). This increased FA and ADC in the acute phase of the ARE model returned to normal in the recovery phase. These data implied that the FA, but not the ADC, reflected the reversibility of vasogenic edema.

In addition to the FA, the diffusion tensor contains other information that allows for further characterization of tissue microstructural alterations during vasogenic edema. These consist of the axial (AD), radial (RD) and mean diffusivities (MD = ADC) (Figure 6(a)),[9] which are calculated by diagonalizing the diffusion tensor to produce its eigenvalues (λ_1, λ_2, and λ_3). The AD (λ_1) is assumed to be parallel to the axonal orientation. The FA is the degree of diffusion anisotropy calculated by using the DT eigenvalues: the FA value is 0 for isotropic diffusion, i.e. in the free water in the brain ventricles. Conversely, the FA value increases up to a maximum of 1.0 when the eigenvalues are significantly different from each other in magnitude.[9]

We found that the AD, but neither the MD nor the RD, increased in our acute ARE model (Figure 6(b) to (e), data not shown for MD). On the other hand, all the diffusivities, AD, MD, and RD, increased in the UCAO-JPD model (Figure 6(c) and (e), data not shown for MD), suggesting the presence of demyelination and/or axonal damage in this model that is distinct from the ARE model.[9] A biplot display of our principal component analysis (Figure 6(f)) revealed that the AD value distinguished our acute ARE model from the controls, after the exclusion of the UCAO-JPD model by its MD and RD. The observed

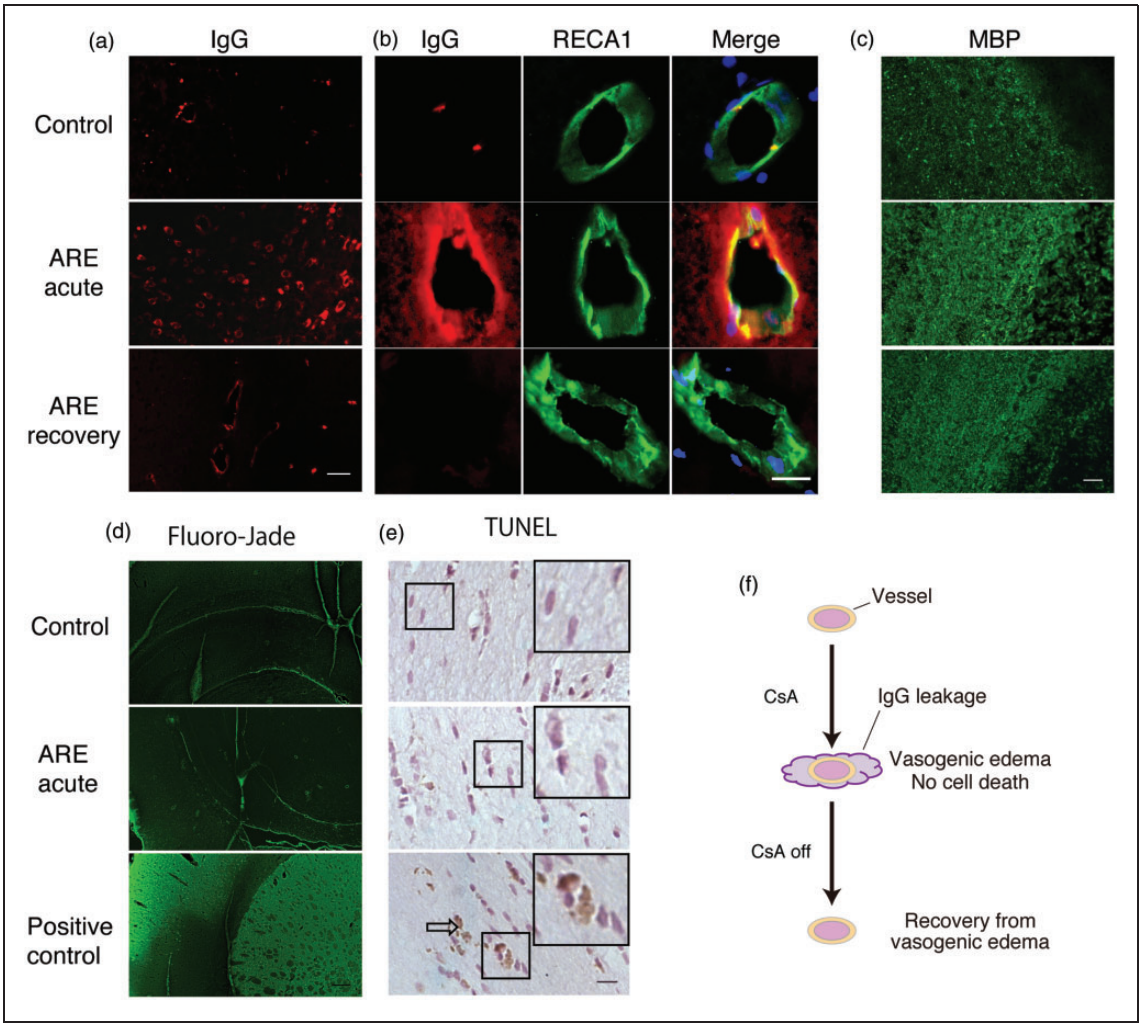

Figure 4. Brain lesions of ARE model revealed IgG leakage without apparent demyelination nor cell death. (a) IgG leakage seen in ARE model. Upper panels, lower magnification views of left corpus callosum and visual cortex from acute- and recovery-phase ARE and control animals. Leaked IgG was taken up by oligodendrocytes and astrocytes in acute ARE. (b) Higher magnification views of IgG leakage in left corpus callosum. IgG leaked outside the vessel in acute ARE (middle column). Green, RECA-1, a marker of endothelial cells; blue, DAPI was used for nuclei. (c) MBP, a marker for myelin and mature oligodendrocytes, staining of corpus callosum from acute- and recovery phase ARE and control animals. (d, e) F&J staining of left cortex (d) and TUNEL staining of corpus callosum (e), of acute-phase ARE and control. Rat brain sections subjected to MCAO were used as positive controls for F&J and nuclease-treated brains for TUNEL. (f) Model of reversible IgG leakage by the stimulated by CsA injections. Scale bars indicate (a, b, e) 20 μm, (c) 200 μm, and (d) 400 μm.

ARE: acute reversible encephalopathy; RECA-1: rat anti-endothelial cell antibody-1; MBP: myelin basic protein; MCAO: middle cerebral artery occlusion; F&J: Fluoro-Jade.

diffusivity differences between these two models represent difference in the profiles of myelination; leaked fluid can diffuse only in the direction parallel to axons in acute ARE because of the limited space in the presence of myelin, whereas it can freely diffuse in demyelinated space in the UCAO-JPD model. This anisotropic diffusion is the cause of the FA increase detected in acute ARE, while increased isotropic diffusion led to an FA decrease in the UCAO-JPD model. The AD increase seen in the acute phase of ARE returned to normal in the recovery phase of ARE.

These results suggest that fluid leakage in vasogenic edema is the cause of the FA increase in white matter without demyelination. The increased axial, but not radial, diffusivity due to IgG leakage in the myelinated space causes the FA to increase in acute ARE.

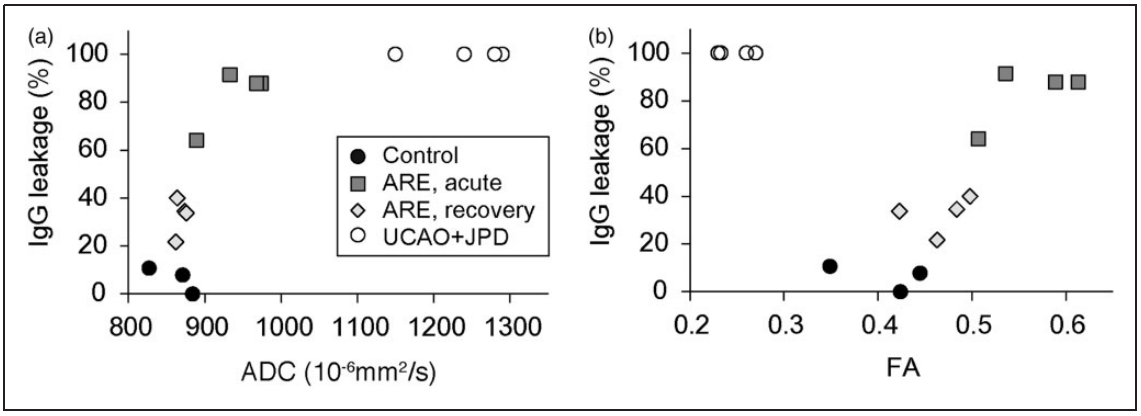

Figure 5. Relationship between histological and diffusion MR data for vasogenic edema in matched brain slices. Scatter plots of IgG leakage area and either (a) ADC or (b) FA values in left corpus callosum of acute- and recovery-phase ARE, UCAO-JPD, and control. MR: magnetic resonance; ADC: apparent diffusion coefficient; FA: fractional anisotropy; UCAO-JPD: unilateral carotid arterial occlusion–Japanese permissive diet.

Although the mechanism is unclear, the increase of AD without significant changes in RD was also seen in gray matter of the acute ARE model.

Discussion

In this study, we used MRI and histology to demonstrate that IgG leakage out of the vessels paralleled an FA increase during the acute phase of reversible vasogenic brain edema induced by CsA in rats. Increased axial, but not radial, diffusivity of water due to leakage into the myelinated space was the cause of this observed FA increase in our ARE model. The present ARE model showed FA increases in both white and gray matter in the absence of demyelination. The FA and IgG leakage returned to normal values upon resolution of the encephalopathy.

Most of the DTI studies reported thus far for various brain injuries in patients and in animal models have reported a decrease in FA.[10,11,13,28] These decreases in the FA were attributed to the demyelination and/or axonal damage present in several disease states and models of chronic white matter injuries, i.e. stroke, small vessel disease, multiple sclerosis, amyotrophic lateral sclerosis and traumatic brain injury.[10,11,26,29–32]

On the other hand, a limited number of studies have reported an FA increase. These could previously be divided into two pathophysiological categories. The first consists of studies finding an FA increase along with a decrease in the ADC, as seen, for example, in cytotoxic edema resulting from the hyper acute stage of stroke (within 3 to 4.5 h from stroke onset). The second category is characterized by findings of an FA increase and only a slight increase in the ADC, as observed in mild traumatic brain injury patients due to astrocytosis.[13,30,31,33,34] The simultaneous significant increases of the FA and the ADC, found, in the absence of demyelination, during the vasogenic edema of the present ARE model, clearly distinguish it from other vasogenic edemas which display a decreased FA accompanied by demyelination. This FA increase accompanied by fluid leakage in the ARE model forms a third pathophysiological category alongside the previous two pathologies that show an increase in the FA. Although our ARE model showed slight astrocytosis both in acute and recovery phases, rather increasing number of these reactive astrocytes at the recovery phase could discriminate the possible contribution of astrocytosis to this FA increase.

Here, we propose a leakage hypothesis, based on water leakage, to explain the FA changes seen in reversible vasogenic edema in our ARE model. As shown in Figure 5, increases in both the ADC and the FA correlated with the severity of the IgG leakage in our ARE model. We suggest that these findings result from the leakage from blood vessels of plasma components (water) that accumulate between the myelin sheaths and compress the myelinated axons. This restricts the diffusion of water perpendicular to the axon forcing the water to move parallel to the axon (Figure 6(g)). The reversibility of the IgG leakage was also confirmed by normalization of the FA and the ADC.

However, in irreversible vasogenic edema with demyelination, i.e. the UCAO-JPD model, the FA does not follow this same pattern with the IgG leakage. An increase in the RD and an FA decrease measured by DTI has been reported to reflect dysmyelination and demyelination and/or axonal damage.[9,35] We propose that this different behavior of the FA value in irreversible vasogenic edema is because the FA change is induced by other histological changes; i.e. demyelination and/or axonal damage. In the presence of

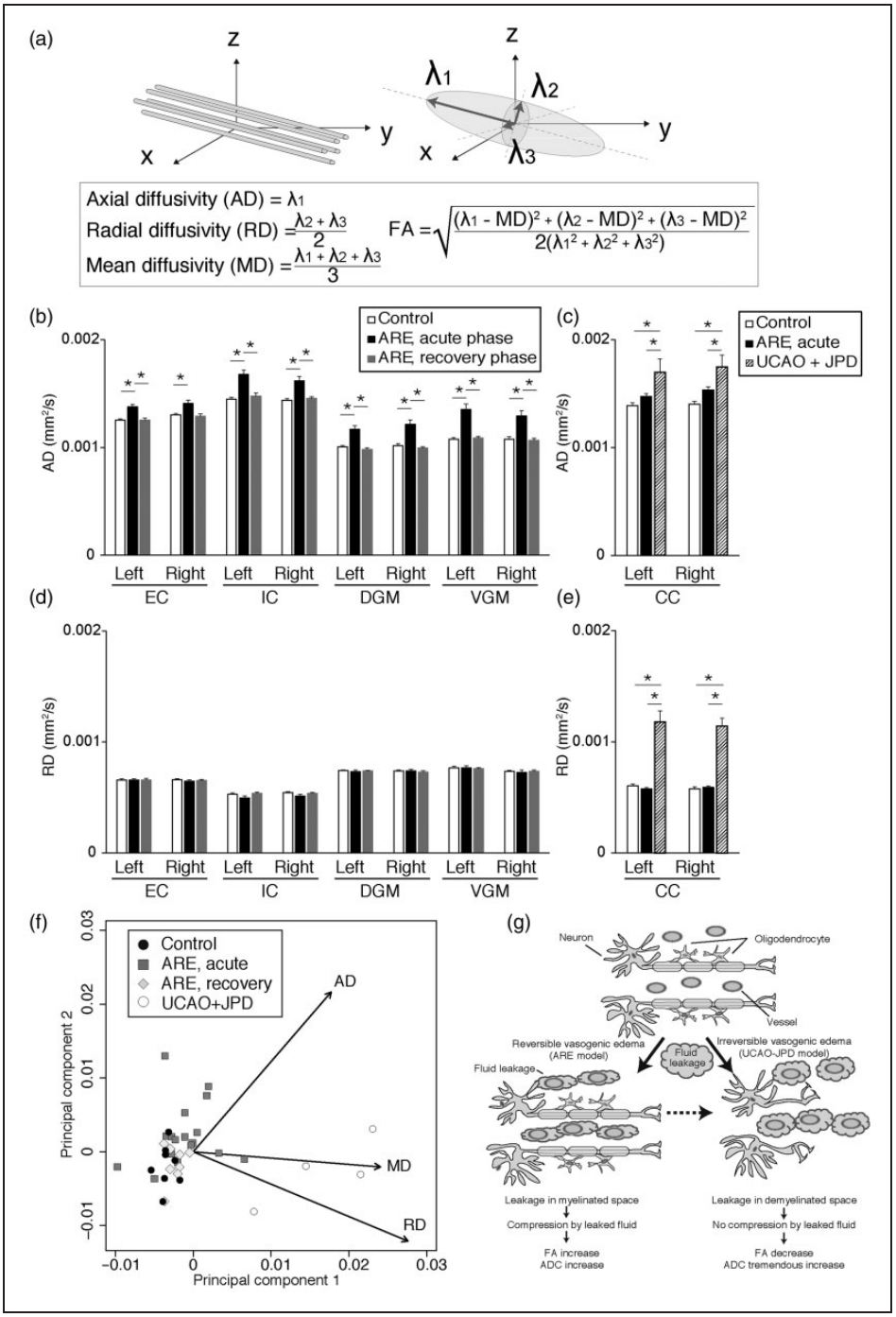

Figure 6. Increased axial, but not radial, diffusivity due to IgG leakage is the cause of FA increase in acute ARE. (a) Schematic representation of MRI parameters. Left: axonal direction of the real world. Right: diffusion tensor. λ_1, λ_2, λ_3; eigenvalues calculated by diagonalization. Of note, λ_1 is the major eigenvalue and its corresponding eigenvector is assumed to be parallel to the axonal orientation. Equations for AD, RD, MD, and FA are shown. (b–e) AD (b and c) and RD (d and e) values in white matter and gray matter from acute- and recovery-phase of ARE model, UCAO-JPD, and their control. (f) A biplot visualization of AD, RD, and MD for ARE, UCAO-JPD, and control. (g) A model for the microstructural changes of brain white matter in reversible and irreversible vasogenic edema (leakage hypothesis). In reversible vasogenic edema fluid leaked from vessels compresses the myelin structures. Then diffusivities perpendicular to axons (RD) decrease and diffusivity parallel to axons increases. This results in an FA increase. In irreversible vasogenic edema, degradation of myelin structures expands the spaces between axons. This results in an increase in the diffusivities in all directions, and therefore, results in FA decrease. The dashed arrow indicates our postulated prognosis in the absence of intervention.

FA: fractional anisotropy; ARE: acute reversible encephalopathy; MRI: magnetic resonance imaging; AD: axial diffusivity; RD: radial diffusivity; MD: mean diffusivity; UCAO-JPD: unilateral carotid arterial occlusion–Japanese permissive diet.

demyelination or axonal damage, the space between the myelin sheaths and fibers expands and water's diffusion becomes more isotropic, leading to a decrease in the FA and an increase in the RD, as seen in our UCAO-JPD model. In addition, due to the enlarged space, IgG leakage does not contribute to this increased water diffusivity (Figure 6(g)).

Taken together, our observations in the present ARE model of an invariant RD together with an FA/ADC increase provide additional support for our hypothesis. The increased FA in the ARE model results from directionally constrained fluid movement within the intact axonal myelin structure. Although not significant, the white matter in our ARE model showed a small, but consistent RD decrease in the acute-phase. We suggest that the RD decreases because fluid leakage compresses the axon, restricting diffusion of water perpendicular to axon and lowering the two radial diffusion tensor eigenvalues, λ_2, λ_3. This phenomenon was also observed during the cytotoxic edema accompanying the hyper acute-phase of stroke.[12] The observed normalization of the FA values in the recovery phase of our ARE model also supports this leakage hypothesis; the FA returns to normal when the leaked plasma components are reabsorbed in the absence of demyelination, cell degeneration, or proliferation.

There are interesting clinical implications of this present study. We propose that FA images could be usefully added to the conventional MRI protocol to discriminate the hyper acute phase from the chronic phase in the cytotoxic edema arising from a stroke.[31] FA images could also be valuable for differentiating the reversible from the irreversible stages in vasogenic edema (Supplementary Table 1). For example, vasogenic edema is the pathogenesis of penumbrae in stroke, while cytotoxic edema is the main pathogenesis of its injured core area.[36] Furthermore, MS/VCI are basically chronic diseases and clinically modified their courses, however, vasogenic edema is the acute pathogenesis of these diseases. Thus, this ARE study is focused on the most important lesions and time course of strokes, MS/VCI and other neurological diseases. Similar FA increases are found in both hyper acute cytotoxic edema and reversible vasogenic edema. However, the behavior of the ADC differs and these differences are clinically used to discriminate vasogenic edema from cytotoxic edema.[8] Clinically, the hyper acute stage of stroke, within the golden hour, and PRES are in this category.

On the other hand, cases where the FA decreases include the chronic stage of cytotoxic edema and irreversible vasogenic edema; both of these situations involve demyelination, axonal damage and a poor prognosis. Clinical examples of these conditions are, for the former, the chronic stage of stroke core lesions, and for the latter, chronic white matter disease and chronic multiple sclerosis lesions. The present ARE model and the UCAO-JPD model are representative animal models for these prognostically opposite vasogenic edemas; acute reversible and chronic irreversible, respectively. Unlike cytotoxic edema, these two conditions in vasogenic edema have not been proved to be chronologically linked. We propose that, in the absence of intervention, reversible vasogenic edema will progress to irreversible edema (dashed arrow in Figure 6(g)).

Although the mechanism proposed above for the increase in FA in the white matter appears to be sound, the FA increase found in the gray matter is more difficult to explain. Other investigators have reported that the FA increased in the gray matter of the basal ganglia in a patient with a subdural hematoma; this FA increase resolved after evacuation of the hematoma.[37] In cases of mild traumatic brain injury in humans and in animal models, the FA also increased in the cortex of the pertinent lesion.[15,38] The proposed mechanisms were compression by the hematoma for the former case and gliosis for the latter. In our ARE model, we found only a slight astrocytosis, which did not resolve with the normalization of the FA increase, suggesting that gliosis per se was not a likely reason for the FA increase. Therefore, we propose that the FA increase seen in the gray matter of our ARE model is due to compression from edematous white matter. This proposal is supported by our observation that the most severe reversible FA increases were mainly seen next to the boundary of the skull (data not shown).

Our established ARE model recapitulated many salient features of human PRES. Seizures are a major manifestation of PRES.[27,39] Most of these patients fully recovered without sequelae.[40,41] Autopsy studies of PRES patients showed several histological manifestations that were very similar to those found in our ARE model. These include an opening of the BBB, reactive astrocytosis, microglial activation, and demyelination without a loss of oligodendrocytes, or no demyelination.[27] MRI studies of PRES patients have also revealed characteristics of reversible vasogenic edema congruent with our findings in the present ARE model; hyperintensities are seen in T_2w MR images along with concomitant increases in the ADC, most prominently in the occipital or occipito-parietal lobes,[5,42] and a narrowing or beaded appearance for the vessels in MRA, reflecting an underlying vasospasm and/or vasoconstriction.[40,41,43] The distribution of lesions in the present ARE model was primarily diffuse, but tended to favor the occipito-parietal area (Bregma -4 to -6 mm). Although it is not clearly identified, both PRES and ARE are likely to be based on the

similar pathogenesis (endothelial damage) due to hypertension and CsA.[7,44,45] Taken together, the features of our model presented a reversible vasogenic edema which closely resembled PRES. Although, to our knowledge, FA images in PRES patients have yet to be reported, an FA increase with subsequent resolution was detected with our model, and we believe that it would be worth searching for a similar reversible FA increase in PRES patients.

We demonstrated that the fluid leakage due to vasogenic edema was the cause of the FA increase observed in white matter, and that this leakage, along with the symptoms, histological and MRI findings was reversible. The ability to detect this reversible vasogenic edema with MR-DTI could enable clinicians to locate areas of the brain for which intervention and rescue may be possible, such as areas in the penumbra of a stroke and in encephalopathy/encephalitis lesions. Our findings herein provide the information that an FA increase in brain white matter is a marker for reversibility and conserved myelination.

Funding

The author(s) disclosed receipt of the following financial support for the research, authorship, and/or publication of this article: GAR was supported by the NINDS (RO1 NS045847). TK was supported by Manpei Suzuki Diabetes Foundation and Uehara Memorial Foundation.

Declaration of conflicting interests

The author(s) declared no potential conflicts of interest with respect to the research, authorship, and/or publication of this article.

Authors' contributions

SK conceived, designed the studies and wrote the manuscript. SK performed behavioral, biochemical, and histologic studies, MRI scans and data analysis. YY, JFT, MC, and VMS performed behavioral, biochemical, and histologic studies and manuscript editing. YrY and LOS performed MRI scans, data analysis, and manuscript editing. TK also designed a portion of the studies and wrote portions of the manuscript. YY and GAR provided scientific advice in the execution of the study and in writing the manuscript.

Supplementary material

Supplementary material for this paper can be found at http://jcbfm.sagepub.com/content/by/supplemental-data

References

1. Liang D, Bhatta S, Gerzanich V, et al. Cytotoxic edema: mechanisms of pathological cell swelling. *Neurosurg Focus* 2007; 22: E2.
2. Rosenberg GA. Neurological diseases in relation to the blood-brain barrier. *J Cerebr Blood Flow Metab* 2012; 32: 1139–1151.
3. Rosenberg GA. Matrix metalloproteinases biomarkers in multiple sclerosis. *Lancet* 2005; 365: 1291–1293.
4. Yang Y and Rosenberg GA. Blood-brain barrier breakdown in acute and chronic cerebrovascular disease. *Stroke* 2011; 42: 3323–3328.
5. Bartynski WS. Posterior reversible encephalopathy syndrome, part 1: fundamental imaging and clinical features. *AJNR Am J Neuroradiol* 2008; 29: 1036–1042.
6. Hugonnet E, Da Ines D, Boby H, et al. Posterior reversible encephalopathy syndrome (PRES): features on CT and MR imaging. *Diagn Interv Imaging* 2013; 94: 45–52.
7. Bartynski WS. Posterior reversible encephalopathy syndrome, part 2: controversies surrounding pathophysiology of vasogenic edema. *AJNR Am J Neuroradiol* 2008; 29: 1043–1049.
8. Newcombe VF, Williams GB, Outtrim JG, et al. Microstructural basis of contusion expansion in traumatic brain injury: insights from diffusion tensor imaging. *J Cerebr Blood Flow Metab* 2013; 33: 855–862.
9. Alexander AL, Lee JE, Lazar M, et al. Diffusion tensor imaging of the brain. *Neurotherapeutics* 2007; 4: 316–329.
10. Lawrence AJ, Chung AW, Morris RG, et al. Structural network efficiency is associated with cognitive impairment in small-vessel disease. *Neurology* 2014; 83: 304–311.
11. Guo AC, MacFall JR and Provenzale JM. Multiple sclerosis: diffusion tensor MR imaging for evaluation of normal-appearing white matter. *Radiology* 2002; 222: 729–736.
12. Song SK, Sun SW, Ju WK, et al. Diffusion tensor imaging detects and differentiates axon and myelin degeneration in mouse optic nerve after retinal ischemia. *Neuroimage* 2003; 20: 1714–1722.
13. Sotak CH. The role of diffusion tensor imaging in the evaluation of ischemic brain injury—a review. *NMR Biomed* 2002; 15: 561–569.
14. Alba-Ferrara LM and de Erausquin GA. What does anisotropy measure? Insights from increased and decreased anisotropy in selective fiber tracts in schizophrenia. *Front Integr Neurosci* 2013; 7(9): 1–5. DOI: 10.3389/fnint.2013.00009.
15. Budde MD, Janes L, Gold E, et al. The contribution of gliosis to diffusion tensor anisotropy and tractography following traumatic brain injury: validation in the rat using Fourier analysis of stained tissue sections. *Brain* 2011; 134: 2248–2260.
16. Alvarez Arroyo MV, Suzuki Y, Yague S, et al. Role of endogenous vascular endothelial growth factor in tubular cell protection against acute cyclosporine toxicity. *Transplantation* 2002; 74: 1618–1624.
17. Luke DR, Brunner LJ and Vadiei K. Bioavailability assessment of cyclosporine in the rat. Influence of route of administration. *Drug Metab Dispos* 1990; 18: 158–162.
18. Jalal FY, Yang Y, Thompson J, et al. Myelin loss associated with neuroinflammation in hypertensive rats. *Stroke* 2012; 43: 1115–1122.

19. Yang Y, Estrada EY, Thompson JF, et al. Matrix metalloproteinase-mediated disruption of tight junction proteins in cerebral vessels is reversed by synthetic matrix metalloproteinase inhibitor in focal ischemia in rat. *J Cerebr Blood Flow Metab* 2007; 27: 697–709.
20. Petullo D, Masonic K, Lincoln C, et al. Model development and behavioral assessment of focal cerebral ischemia in rats. *Life Sci* 1999; 64: 1099–1108.
21. Mountney A, Leung LY, Pedersen R, et al. Longitudinal assessment of gait abnormalities following penetrating ballistic-like brain injury in rats. *J Neurosci Methods* 2013; 212: 1–16.
22. Liu Y, Ao LJ, Lu G, et al. Quantitative gait analysis of long-term locomotion deficits in classical unilateral striatal intracerebral hemorrhage rat model. *Behav Brain Res* 2013; 257: 166–177.
23. Chen YJ, Cheng FC, Sheu ML, et al. Detection of subtle neurological alterations by the Catwalk XT gait analysis system. *J Neuroeng Rehabil* 2014; 11(62): 1–13.
24. Schmued LC, Stowers CC, Scallet AC, et al. Fluoro-Jade C results in ultra high resolution and contrast labeling of degenerating neurons. *Brain Res* 2005; 1035: 24–31.
25. Gabriel KR. The biplot graphic display of matrices with application to principal component analysis. *Biometrika* 1971; 58: 453–467.
26. Jalal FY, Yang Y, Thompson JF, et al. Hypoxia-induced neuroinflammatory white-matter injury reduced by minocycline in SHR/SP. *J Cerebr Blood Flow Metab* 2015; 35(7): 1145–1153.
27. Singh N, Bonham A and Fukui M. Immunosuppressive-associated leukoencephalopathy in organ transplant recipients. *Transplantation* 2000; 69: 467–472.
28. Bendlin BB, Ries ML, Lazar M, et al. Longitudinal changes in patients with traumatic brain injury assessed with diffusion-tensor and volumetric imaging. *Neuroimage* 2008; 42: 503–514.
29. Aoki S, Iwata NK, Masutani Y, et al. Quantitative evaluation of the pyramidal tract segmented by diffusion tensor tractography: feasibility study in patients with amyotrophic lateral sclerosis. *Radiat Med* 2005; 23: 195–199.
30. Croall ID, Cowie CJ, He J, et al. White matter correlates of cognitive dysfunction after mild traumatic brain injury. *Neurology* 2014; 83: 494–501.
31. Puig J, Blasco G, Daunis IEJ, et al. Increased corticospinal tract fractional anisotropy can discriminate stroke onset within the first 4.5 hours. *Stroke* 2013; 44: 1162–1165.
32. Yang Y, Salayandia VM, Thompson JF, et al. Attenuation of acute stroke injury in rat brain by minocycline promotes blood-brain barrier remodeling and alternative microglia/macrophage activation during recovery. *J Neuroinflamm* 2015; 12(26): 1–5.
33. Yang Q, Tress BM, Barber PA, et al. Serial study of apparent diffusion coefficient and anisotropy in patients with acute stroke. *Stroke* 1999; 30: 2382–2390.
34. Ling JM, Pena A, Yeo RA, et al. Biomarkers of increased diffusion anisotropy in semi-acute mild traumatic brain injury: a longitudinal perspective. *Brain* 2012; 135: 1281–1292.
35. Song SK, Sun SW, Ramsbottom MJ, et al. Dysmyelination revealed through MRI as increased radial (but unchanged axial) diffusion of water. *Neuroimage* 2002; 17: 1429–1436.
36. Taheri S, Candelario-Jalil E, Estrada EY, et al. Spatiotemporal correlations between blood-brain barrier permeability and apparent diffusion coefficient in a rat model of ischemic stroke. *PloS One* 2009; 4: e6597.
37. Osuka S, Matsushita A, Ishikawa E, et al. Elevated diffusion anisotropy in gray matter and the degree of brain compression. *J Neurosurg* 2012; 117: 363–371.
38. Bouix S, Pasternak O, Rathi Y, et al. Increased gray matter diffusion anisotropy in patients with persistent post-concussive symptoms following mild traumatic brain injury. *PloS One* 2013; 8: e66205.
39. Endo A, Fuchigami T, Hasegawa M, et al. Posterior reversible encephalopathy syndrome in childhood: report of four cases and review of the literature. *Pediatr Emerg Care* 2012; 28: 153–157.
40. Yasuhara T, Tokunaga K, Hishikawa T, et al. Posterior reversible encephalopathy syndrome. *J Clin Neurosci* 2011; 18: 406–409.
41. Lin JT, Wang SJ, Fuh JL, et al. Prolonged reversible vasospasm in cyclosporin A-induced encephalopathy. *AJNR Am J Neuroradiol* 2003; 24: 102–104.
42. Liu X, Almast J and Ekholm S. Lesions masquerading as acute stroke. *J Magn Reson Imaging* 2013; 37: 15–34.
43. Shbarou RM, Chao NJ and Morgenlander JC. Cyclosporin A-related cerebral vasculopathy. *Bone Marrow Transplant* 2000; 26: 801–804.
44. Bailey EL, Wardlaw JM, Graham D, et al. Cerebral small vessel endothelial structural changes predate hypertension in stroke-prone spontaneously hypertensive rats: a blinded, controlled immunohistochemical study of 5- to 21-week-old rats. *Neuropathol Appl Neurobiol* 2011; 37: 711–726.
45. Yamagata K. Pathological alterations of astrocytes in stroke-prone spontaneously hypertensive rats under ischemic conditions. *Neurochem Int* 2012; 60: 91–98.